

Spin-dependent scattering of boosted dark matter

Wenyu Wang^{1,*} Lei Wu,^{2,†} Wen-Na Yang^{1,4,‡} and Bin Zhu^{3,§}

¹*Faculty of Science, Beijing University of Technology, Beijing 100124, China*

²*Department of Physics and Institute of Theoretical Physics, Nanjing Normal University, Nanjing, 210023, China*

³*School of Physics, Yantai University, Yantai 264005, China*

⁴*School of Fundamental Physics and Mathematical Sciences, Hangzhou Institute for Advanced Study, UCAS, Hangzhou 310024, China
and University of Chinese Academy of Sciences, 100190 Beijing, China*



(Received 29 November 2021; accepted 10 March 2023; published 10 April 2023)

Boosted dark matter is a promising method for probing light dark matter, with a well-developed computational framework for spin-independent scattering already existing. The spin-dependent case, on the other hand, lacks a coherent treatment. We therefore give the first comprehensive derivation of the spin-dependent scattering cross section for boosted dark matter, finding that certain effects can lead to enhanced experimental sensitivity compared to the conventional contact interaction. For example, when the transfer momentum is sufficiently large, the time component of the dark matter current contributes significantly to the proton structure factor. Also, even without a light mediator, we find a residual momentum dependence in the quark-nucleon matching operation that can contribute similarly. We promote this endeavor by deriving direct limits on sub-GeV spin-dependent scattering of boosted dark matter from terrestrial data. We find that the exclusion limits from the boosted structure factor differ by as much as six orders of magnitude from those calculated using nonrelativistic structure factors.

DOI: [10.1103/PhysRevD.107.073002](https://doi.org/10.1103/PhysRevD.107.073002)

I. INTRODUCTION

Observations in cosmology and astrophysics have supported the presence of dark matter (DM) [1]. Its features, such as mass and interactions are however still unknown. One of the most promising experimental avenues is to search for the small energy depositions from the DM elastically scattering in sensitive detectors on the Earth. Strict constraints exist on the cross section for DM heavier than 1 GeV. As the detection limits reach the neutrino floor, we must look for other strategies to explore the surviving parameter space of DM or find some means to detect DM beyond ordinary considerations [2].

A crucial aspect of the theoretical study of DM detection is the elastic scattering process between DM and the nuclei, which determines detection rates. We can classify the

hypothetical DM-nucleon interactions into the spin-independent and spin-dependent cases. There is already an impressive range of existing constraints on the DM-nucleon cross section in the MeV-to-GeV mass range, ranging from rare processes involving the emission of photons or “Migdal” electrons from the recoiling atom [3–6], and the small flux of boosted dark matter (BDM) arising from interactions between DM and cosmic rays, the Sun, or mesons [7–19]. That said, although there is a well-developed framework for spin-independent scattering of BDM, a thorough treatment for spin-dependent scattering is lacking.

Since weakly interacting massive particles (WIMPs) are heavy, they are estimated to be rotating around our galaxy at a nonrelativistic velocity of several hundred kilometers per second, and with a minimum escape velocity $v_{\text{esc}} \sim 544$ km/s. Therefore nonrelativistic expansions of the DM-nucleon scattering amplitude in powers of the DM-nucleon relative velocity are appropriate for evaluating the cross section [20]. Though the nonrelativistic expansion or the effective field theory is reliable in dealing with WIMP scattering, the neglect of higher-order terms is problematic in some circumstances. For example, in a novel detection of sub-GeV dark matter, called cosmic ray dark matter (CRDM) [8,12,13,19,21–24], this simple expansion is not reliable. This is because that the incident dark matter is boosted to be relativistic, and the momentum transfer q is

*wywang@bjut.edu.cn

†leiwu@njnu.edu.cn

‡Corresponding author.

yangwenna22@mails.ucas.ac.cn

§zhubin@mail.nankai.edu.cn

Published by the American Physical Society under the terms of the Creative Commons Attribution 4.0 International license. Further distribution of this work must maintain attribution to the author(s) and the published article’s title, journal citation, and DOI. Funded by SCOAP³.

comparable to the DM mass in the sub-GeV region, thus the dropped higher-order terms could be significant [25] in the DM-nuclei scattering.

In this work, we focus on spin-dependent boosted dark matter scattering. We assume dark matter is a Majorana fermion for the sake of comparison. This is due to the fact that the Majorana-type DM always occurs in the most popular models of physics beyond the Standard Model, such as those featuring supersymmetry [26] or extra dimensions [27]. It is worth noting that our calculation is not limited to Majorana DM, which can be easily extended to Dirac fermion or scalar DM. Previous calculations of spin-dependent WIMP scattering have started from WIMP-nucleon currents and used the nuclear-structure function to convert the result to the nuclei. However, nuclear structure calculations can be improved with recent advances in nuclear interactions and computing capabilities. We can thus demonstrate the difference between the WIMP-nuclei scattering and boosted DM scattering on the target. Furthermore, we find another source of the momentum transfer effect in the contact interaction, where the finite size proton accounts for the momentum dependent behavior.

II. COMPUTATIONAL FRAMEWORK

In order to demonstrate the subtlety of BDM spin-dependent scattering, we firstly sketch the ordinary computation of the WIMP spin-dependent cross section. At low momentum transfer q , the Lagrangian for the interaction between DM and quarks can be evaluated using chiral effective field theory [28,29]. In the neutron or proton-only case, the differential scattering cross section can be rewritten as [30]

$$\frac{d\sigma^{\text{SD}}}{dq^2} = \frac{\sigma_{\chi N}^{\text{SD}}}{3\mu_N^2 v^2} \frac{\pi}{2J+1} S_A(q), \quad (1)$$

in which μ_N is the reduced mass of the DM-nucleon system, and $\sigma_{\chi N}$ is the scattering cross section between a DM particle and a single proton or neutron at zero momentum transfer. v is the WIMP velocity in the rest frame of the detector, and J is the initial ground-state angular momentum of the nuclei. The total expected nonrelativistic spectrum of the detection rate dR/dE_r is $\frac{dR}{dE_r} = \frac{2\rho_\chi}{m_\chi} \int \frac{d\sigma^{\text{SD}}}{dq^2} v f(\mathbf{v}) d^3v$. m_χ is the mass of the DM, ρ_χ is the local DM density, and $f(\mathbf{v})$ is the velocity distribution in the rest frame of the detector. $q = \sqrt{2E_r m_N}$ is the transfer momentum. If we assume a standard isothermal WIMP halo, then $v_0 = 220$ km/s, $\rho_\chi = 0.3$ GeV/($c^2 \times \text{cm}^3$), $v_{\text{esc}} = 544$ km/s, and Earth velocity $v_E = 232$ km/s. If we generalize the WIMP into BDM, the Maxwell-Boltzmann distribution is replaced by the incoming DM flux $d\Phi_\chi/dE_\chi$.

The structure factor $S_A(q)$ plays a crucial role in determining the event rate of spin-dependent scattering process in both relativistic and nonrelativistic process,

$$S_A(q) = \frac{1}{4\pi G_v^2} \sum_{s_f, s_i} \sum_{M_f, M_i} |\langle f | \mathcal{L}_\chi^{\text{SD}} | i \rangle|^2, \quad (2)$$

in which the sum $s_f, s_i = \pm 1/2$ is over Majorana fermion spin projections, and the sum M_f, M_i is over the projections of the total angular momentum of the final and initial states J_f, J_i . We assume the heavy mediator is a vector so that $G_v \sim 1/m_V^2$. It is easy to include the scalar mediator scenario. Usually, the heavy mediator does not lead to a momentum transfer effect in the scattering process. However, we find there is still a residual momentum transfer effect through the matching procedure from quark to proton. The structure factor has three contributions: the spatial current, temporal current, and interference component current. Fortunately, we find that the wave functions of the spatial current and the temporal current are orthogonal to each other, making their interference terms vanish. One can write the structure factor as

$$S_A(q) = S_A^0(q) + S_T(q), \quad (3)$$

where $S_A^0(q)$ denotes the contribution from the spatial current couplings and $S_T(q)$ is the time component contributions. Evaluating the Lagrangian density between the initial and final state, the spatial contribution is

$$\langle f | \mathcal{L}_\chi^{\text{SD}} | i \rangle = -\frac{G_v}{\sqrt{2}} \int d^3r e^{-iq\mathbf{r}} \bar{\chi}_f \boldsymbol{\gamma} \gamma^5 \chi_i \mathbf{J}_i^A(\mathbf{r}), \quad (4)$$

in which $e^{-iq\mathbf{r}} \bar{\chi}_f \boldsymbol{\gamma} \gamma^5 \chi_i = \langle \chi_f | \mathbf{j}(\mathbf{r}) | \chi_i \rangle$ is the matrix element of the current of the DM and $\mathbf{J}_i^A(\mathbf{r}) = \sum_q A_q \bar{\psi}_q \boldsymbol{\gamma} \gamma^5 \psi_q$ denotes the hadronic current [28]. For the response of the nuclei, the spin-dependent dark matter interaction couples dominantly to a single nucleon, but also to pairs of nucleons. Then the quark currents are replaced by their expectation value in the nucleon, leading to a 1b axial-vector current at one-nucleon level. The DM interaction couples to nucleon pairs at order q^3 . This leads to a 2b axial-vector current. However, the error of the 2b current level results is too large, Thus the 1b current results are used in this work for the simplicity. The structure factor $S_A^0(q)$ can be decomposed as a sum over multipoles L with reduced matrix elements of the longitudinal \mathcal{L}_L^5 , transverse electric $\mathcal{T}_L^{\text{el}5}$, and transverse magnetic $\mathcal{T}_L^{\text{mag}5}$ projections of the axial-vector currents

$$S_A^0(q) = \sum_{L \geq 0} |\langle J_f | \mathcal{L}_L^5 | J_i \rangle|^2 + \sum_{L \geq 1} (|\langle J_f | \mathcal{T}_L^{\text{el}5} | J_i \rangle|^2 + |\langle J_f | \mathcal{T}_L^{\text{mag}5} | J_i \rangle|^2). \quad (5)$$

For fast-moving DM, the projections of the axial-vector currents will not be changed but become dependent on the momentum of the incident DM particle

$$\begin{aligned}
S_A^0(q, p_i, p_f) &= \frac{1}{2} \left[\sum_{L \geq 0} \frac{1}{E_f E_i} (2p_f^3 p_i^3 + p_f \cdot p_i + m_\chi^2) |\langle J_f | \mathcal{L}_L^5 | J_i \rangle|^2 \right. \\
&+ \sum_{L \geq 1} \frac{1}{E_f E_i} (p_f^1 p_i^1 + p_f^2 p_i^2 + p_f \cdot p_i + m_\chi^2) \\
&\times \left. \left(|\langle J_f | \mathcal{T}_L^{\text{el}5} | J_i \rangle|^2 + |\langle J_f | \mathcal{T}_L^{\text{mag}5} | J_i \rangle|^2 \right) \right]. \quad (6)
\end{aligned}$$

We can also get the time component contribution to the structure factor¹

$$\begin{aligned}
S_T(q) &= \frac{1}{4E_i E_f} \frac{1}{4E'_i E'_f} \frac{1}{2\pi} \left[4 \left(2E_i E_f - \frac{q^2}{2} - 2m_\chi^2 \right) \right. \\
&\times \left(2E'_i E'_f - \frac{q^2}{2} - 2m_N^2 \right) \\
&+ 4 \frac{m_N}{q^2 + m_\pi^2} \left(2E_i E_f - \frac{q^2}{2} - 2m_\chi^2 \right) (E'_i - E'_f) m_N q_0 \\
&\left. + \left(\frac{m_N}{q^2 + m_\pi^2} \right)^2 \left(2E_i E_f - \frac{q^2}{2} - 2m_\chi^2 \right) \frac{q^2}{2} q_0^2 \right]. \quad (7)
\end{aligned}$$

We can make some general comments about the boosted structure factor before concluding this section. The spatial and time components of the structure factor for semi-relativistic kinematics are not a function of q only, but instead the incoming dark matter momentum p_i or kinetic energy T_χ . To obtain an effective structure factor, we need to integrate out the phase space of incoming momentum

$$S_{\text{eff}}(q) = \int dT_\chi \frac{d\Phi_\chi}{dT_\chi} S(T_\chi, q). \quad (8)$$

This is equivalent to the conventional Maxwell-Boltzmann velocity integral when the incoming DM momentum reduces to the nonrelativistic regime.

To get some feeling for this modification, we choose two specific collisions to obtain the corresponding structure factors for the demonstration. The first one is $p_i = (E_i, 0, 0, p_i)$, $p_f = (E_f, p_f, 0, 0)$, $p'_i = (m_N, 0, 0, 0)$, $p'_f = (E'_f, -p_f, 0, p_i)$. In this case, the final direction of scattering DM is perpendicular to the collision axis (vertical ejection). And the structure factors (with a superscript tag \perp) are

$$\begin{aligned}
S_A^{\perp}(q) &= \frac{4m_\chi^2 + q^2}{4m_\chi^2 + 2q^2} \sum_{L \geq 0} |\langle J_f | \mathcal{L}_L^5 | J_i \rangle|^2 \\
&+ \frac{4m_\chi^2 + q^2}{4m_\chi^2 + 2q^2} \sum_{L \geq 1} |\langle J_f | (\mathcal{T}_L^{\text{el}5} + \mathcal{T}_L^{\text{mag}5}) | J_i \rangle|^2, \quad (9)
\end{aligned}$$

$$\begin{aligned}
S_T^{\perp}(q) &= \frac{1}{8\pi} \frac{1}{2m_\chi^2 + q^2} \frac{1}{2m_N^2 + q^2} \\
&\times \left[q^4 - \frac{1}{2} \frac{q^6}{q^2 + m_\pi^2} + \left(\frac{1}{q^2 + m_\pi^2} \right)^2 \frac{q^8}{16} \right]. \quad (10)
\end{aligned}$$

Another collision is $p_i = (E_i, 0, 0, p_i)$, $p_f = (E_f, 0, 0, -p_i)$, $p'_i = (m_N, 0, 0, 0)$, $p'_f = (E'_f, 0, 0, 2p_i)$, which is the backward scattering in case of the heavy target nuclei. Then the structure factors (with a superscript tag \triangleleft) are

$$\begin{aligned}
S_A^{\triangleleft}(q) &= \frac{4m_\chi^2}{4m_\chi^2 + q^2} \sum_{L \geq 0} |\langle J_f | \mathcal{L}_L^5 | J_i \rangle|^2 \\
&+ \sum_{L \geq 1} |\langle J_f | (\mathcal{T}_L^{\text{el}5} + \mathcal{T}_L^{\text{mag}5}) | J_i \rangle|^2, \quad (11)
\end{aligned}$$

$$S_T^{\triangleleft}(q) = 0. \quad (12)$$

The differences between nonrelativistic and boosted structure factors are shown in Fig. 1 in which the DM mass are chosen as $m_\chi = 1$ MeV (left) and $m_\chi = 100$ MeV for the comparison. The upper two panels are the results of vertical ejection of dark matter at the 1b current level. The black solid lines show the structure factor of the WIMP DM. The red solid lines show the new structure factors obtained by considering both the time component and the spatial contribution of the axial current in the case of boosted scattering between the DM and the nuclei. The pink dotted lines are the spatial component contribution and the blue dotted lines are the time component contribution. The lower two panels are the results of backward scattering at the 1b current level. Similar to the upper panels, the red solid lines show the new structure factor which only comes from the spatial contribution. From the numerical results shown in the figure, we can see that when the DM mass become much less than the GeV WIMP, the structure factors are suppressed (see the left 1 MeV panels) in the small transfer momentum region. This is due to the momentum dependent coefficients in Eq. (6). Though the time component contribution are negligible in the small transfer momentum region, it can be dominant in the large transfer momentum region and it can enhance the factors to a big value when q is sufficiently large. Note that this time component contribution dominant region is beyond the ordinary detection region of the recoil energy ($u \ll 1$) in typical DM detectors.

¹Note that we choose the time component contribution at the nucleon level to account for the nuclear contributions to the structure factor. A detailed deviation can be found in the Appendix C.

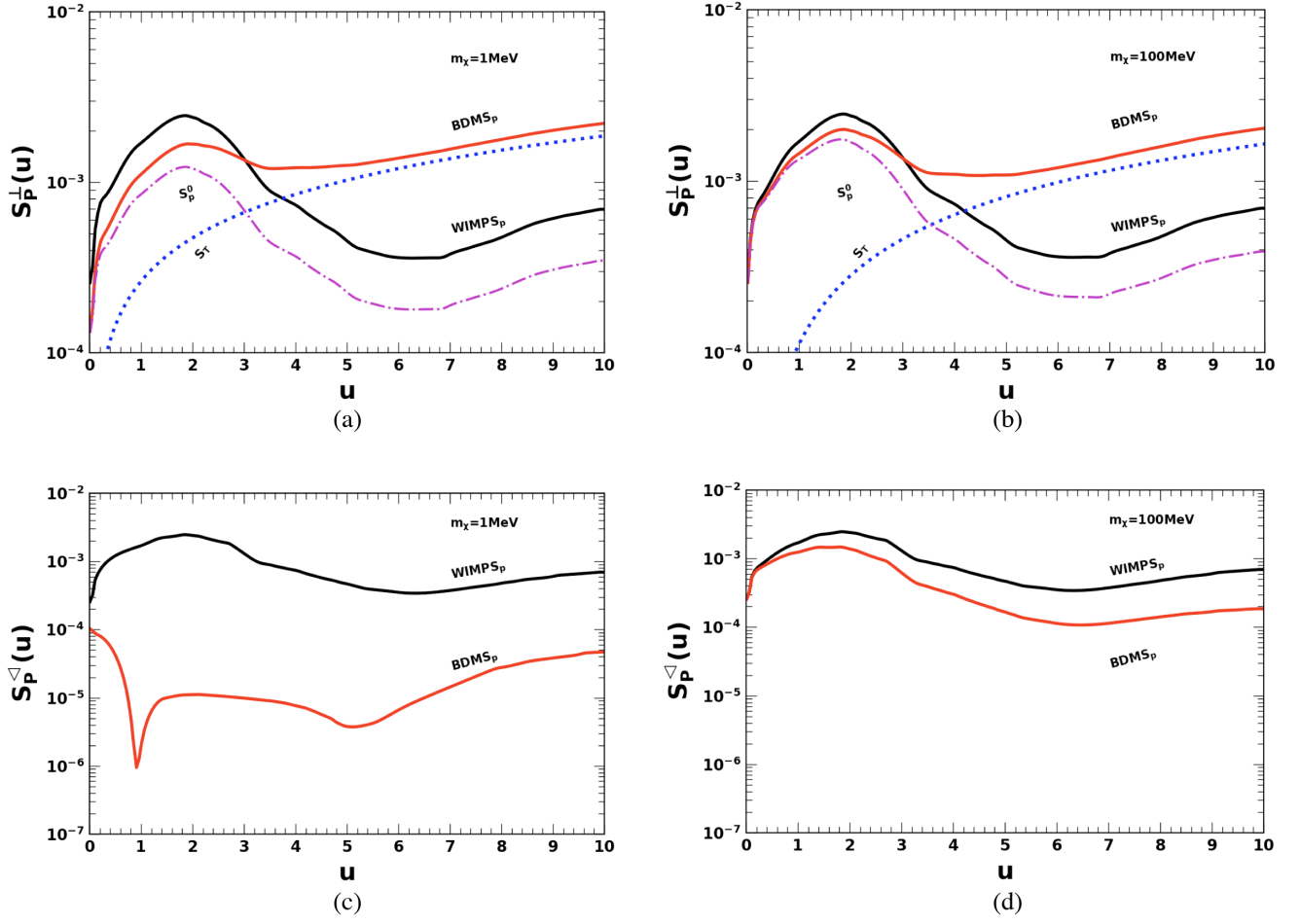


FIG. 1. Structure factors $S_p(u)$ for Xe^{131} as a function of $u = q^2 b^2 / 2$, the harmonic-oscillator lengths are $b = 2.2905$ fm. The upper two panels with $m_\chi = 1$ MeV (left) and $m_\chi = 100$ MeV (right) are the results of vertical ejection of dark matter at the 1b current level. The black solid lines show the structure (WIMP) factor of the WIMP DM case. The red solid lines show the new structure (BDM) factor obtained by considering both the time component and the spatial contribution of the axial current in the case of boosted scattering between the DM and the nuclei. The pink dotted lines are the spatial component contribution and the blue dotted lines are the time component contribution. The lower two panels with $m_\chi = 1$ MeV (left) and $m_\chi = 100$ MeV (right) are the results of backward scattering at the 1b current level. The black solid lines show the structure (WIMP) factor of the WIMP DM case. The red solid lines show the new structure (BDM) factor obtained by considering both the time component and the spatial contribution of the axial current in the case of boosted scattering between the DM and the nuclei. Note that the time component is zero and the total contribution comes from the spatial part.

The momentum dependent coefficients generally suppress the spatial contribution of the new structure factor. The upper left panel shows that the spatial contribution is about one-half of the WIMP structure factor. However, in the backward scattering, the spatial contribution of the new structure factor can be three orders of magnitude lower than WIMP structure factor. The reason can be easily derived from the momentum dependent coefficients in Eqs. (9)–(12). For example, the longitudinal \mathcal{L}_L^5 in Eq. (11) is greatly suppressed when the DM mass is negligible compared to transfer momentum. This implies that the large angle scattering provides a much greater suppression factor than vertical eject scattering. As shown in the following section, the large angle scattering

will become significantly important in the study of the boosted dark matter.

In addition, the structure factors are derived from the four-fermion compact interactions. As a result, it is natural to disregard the momentum dependence of the DM, i.e., $F_{\text{DM}} = 1$. In spin-dependent scattering, however, the matching between quarks and nucleons gives residual momentum dependence via pion exchange $b_1 = m_N a_1 / (m_\pi^2 + q^2)$. We give a detailed calculation of the nucleon matrix elements and a detailed description of b_1 in Appendix C. Such an effect does not come from the light mediator exchange but rather the finite size effect of protons and neutrons.

III. BENCHMARK MODEL: COSMIC-RAY BOOSTED DARK MATTER

In the CRDM scenario, DM is boosted by energetic galactic cosmic rays, and it subsequently becomes a fast-moving particle which is one component of cosmic rays. Following scattering in detectors, new limits on the DM-nucleon scattering cross section below 1 GeV can be obtained. CRs transfer kinetic energy to the static DM particle, making it form an energetic flux. The DM flux in this situation resembles the neutrino flux scattering from outer space, allowing neutrino detectors, such as MiniBooNE *et al.* to give constraints on the CRDM parameter space. This relativistic DM flux can be obtained via the collision rate of CRs with DM per unit kinetic energy of CRs (T_i) and DM (T_χ) in a differential volume dV

$$\frac{d^2\Gamma_{\text{CR}_i \rightarrow \chi}}{dT_i dT_\chi} = \frac{\rho_\chi}{m_\chi} \frac{d\sigma_{\chi i}}{dT_\chi} \frac{d\Phi_i^{\text{LIS}}}{dT_i} dV, \quad (13)$$

where the flux is taken in the local interstellar (LIS) population of the CRs [31], and i stands for the specific species of the cosmic rays. Integrating this over the relevant volume and CR energies yields a boosted DM flux

$$\begin{aligned} \frac{d\Phi_\chi}{dT_\chi} &= \int_{\Omega} \frac{d\Omega}{4\pi d^2} \int_{T_{\text{min}}} dT_i \frac{d^2\Gamma_{\text{CR}_i \rightarrow \chi}}{dT_i dT_\chi}, \\ &= D_{\text{eff}} \frac{\rho_\chi}{m_\chi} \sum_i \int_{T_{\text{min}}} dT_i \frac{d\sigma_{\chi i}}{dT_\chi} \frac{d\Phi_i^{\text{LIS}}}{dT_i}. \end{aligned} \quad (14)$$

Since incoming proton CRs are highly relativistic, the structure factor reduces to 1. When the CRDM particle travels from the upper atmosphere to the detector, the scattering with dense matter attenuates the flux to zero, which explains why CRDM searches are sometimes blind to large cross sections: large scattering cross sections generally give a large CRDM flux, however this also leads to a significant attenuation of the flux. The degradation of the energy of the CRDM component can be expressed via

$$\frac{dT_\chi}{dx} = - \sum_N n_N \int_0^{E_r^{\text{max}}} \frac{d\sigma_{\chi N}}{dE_r} E_r dE_r. \quad (15)$$

Here, E_r refers to the energy loss by a CRDM particle in a collision with a nuclei N . $d\sigma_{\chi N}/dE_r$ is the differential cross section of DM scattering on dense matter.

Effectively, we can find the CRDM flux at the depth z from the flux at the upper atmosphere via

$$\frac{d\Phi_\chi}{dT_\chi^z} = \left(\frac{dT_\chi}{dT_\chi^z} \right) \frac{d\Phi_\chi}{dT_\chi} = \frac{4m_\chi^2 e^{z/\ell}}{(2m_\chi + T_\chi^z - T_\chi^z e^{z/\ell})^2} \frac{d\Phi_\chi}{dT_\chi}, \quad (16)$$

where $d\Phi_\chi/dT_\chi$ needs to be evaluated at

$$T_\chi = T_\chi^0(T_\chi^z) = 2m_\chi T_\chi^z e^{z/\ell} (2m_\chi + T_\chi^z - T_\chi^z e^{z/\ell})^{-1}. \quad (17)$$

Here ℓ denotes the mean free path of the DM particles, which can be calculated using the scattering cross section and the density of ordinary matter on the Earth,

$$\ell^{-1} \equiv \sum_N n_N \int_0^{E_r^{\text{max}}} dE_r \frac{d\sigma_{\chi N}}{dE_r}, \quad (18)$$

Note that Eq. (16) is valid for the attenuation with a constant cross section. It is only a qualitative description of the differential cross section studied in this paper. The quantitative numerical calculation is implemented according to our model.

CRDM particles can transfer the energy to a target nuclei inside the detector, triggering detection events, just as with ordinary DM direct detection. Therefore there is a natural bridge to reinterpret existing data in the CRDM context. The equivalence between their event rate gives rise to a constraint on the critical values of mass and coupling. For WIMP DM, it can read from experiment directly, while for CRDM

$$R = \int_{T_1}^{T_2} dE_r \frac{1}{m_T} \int_{T_\chi^{\text{min}}}^\infty dT_\chi^z \frac{d\Phi_\chi}{dT_\chi^z} \frac{d\sigma_{\chi T}}{dE_r}, \quad (19)$$

where T_1 and T_2 are the analysis window for the detectors, and the DM differential flux can be regarded as a modification of the velocity distribution $f(\mathbf{v})$. The differential event rate is composed of the flux and differential cross section, and the flux $d\Phi_\chi/dT_\chi^z$ is evaluated at the detector after considering attenuation processes. $d\sigma_{\chi T}/dE_r$ is the differential cross section of DM-nuclei elastic scattering. Note that the mean free path ℓ is calculated in the integrand for every Monte Carlo sample. One can easily check that the dominant component S_A^0 of the structure factor can be written as a function of the energy T_χ^z of the incident DM

$$\begin{aligned} S_A^0 &= \frac{4(T_\chi^z + m_\chi)^2 - q^2}{4(T_\chi^z + m_\chi)^2} \sum_{L \geq 0} |\langle J_f || \mathcal{L}_L^5 || J_i \rangle|^2 \\ &+ \frac{q^2 + 4m_\chi^2}{4(T_\chi^z + m_\chi)^2} \sum_{L \geq 1} (|\langle J_f || \mathcal{T}_L^{\text{el}5} || J_i \rangle|^2 \\ &+ |\langle J_f || \mathcal{T}_L^{\text{mag}5} || J_i \rangle|^2). \end{aligned} \quad (20)$$

Integrating the event rate, we can obtain a relationship between experimental data and theoretical models. In our numerical study, the package DarkSUSY [32,33] is used for simulating CRDM detection. The spin-dependent cross section with the new structure factor are coded in the

version DarkSUSY-6.3.1 [34]. And we checked with our own modified code based on DarkSUSY-6.3.1, of which the results are consistent.

The numerical results of our calculation are shown in the Fig. 2, from which we may conclude the following:

- (1) The upper limits for the two instances considered are the same in the $m_\chi \gtrsim 0.1$ GeV regime because the BDM structure factor recovers the WIMP structure factor when the DM mass is heavier than 1 GeV. We can see that the exclusion regions are distinct below 0.1 GeV, where the BDM limits become much weaker due to the suppression factor added in Eq. (20). Notably, BDM limits can be as much as six orders of magnitude weaker than the results of WIMP structure factor below the MeV mass region. One can analytically derive from Eq. (6) that this much weaker limits mainly come from the large angle scattering of the CRDM, as shown in the above section. The detailed calculations of structure factors can be found in the Supplemental Material.
- (2) It is worth noting that the detection of the recoil energy E_r necessitates a very tiny u , yet the transfer momentum q is sufficient. The maximum E_r (40 KeV), for example, indicates that q is at about 100 MeV. These results reveal that the new spatial

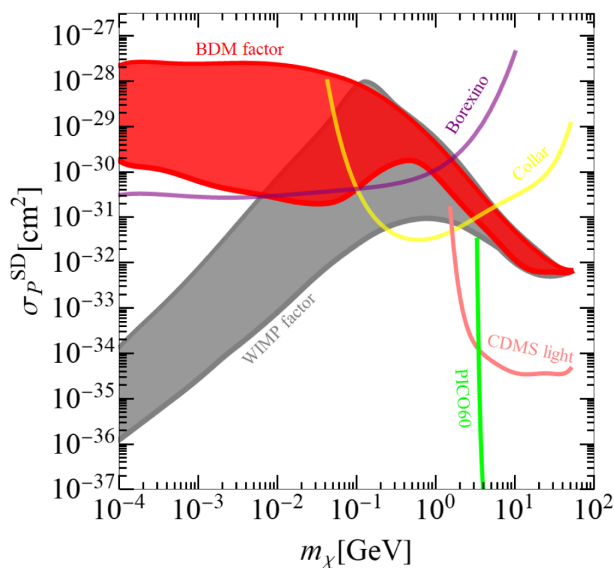


FIG. 2. Limits on the spin-dependent cross section from Xenon1T data. The red area shows the exclusion results using the boosted structure factor derived in this work; the dark gray contour shows the results from the nonrelativistic structure factor. The difference between the two is evidently significant, especially for light DM. For comparison, the limits from the direct detection experiments CDMS light [35], PICO60 [36], and PICASSO [37], Borexino (we can refer to the purple line in Fig. 3 of Ref. [8]) as well as from delayed-coincidence searches in near-surface detectors by Collar [38] are also shown in the plot.

contribution to the structure factor is critical in the evaluation of the spin-dependent scattering between DM and nuclei.

- (3) Another point to note is that the exclusion regions are similar whether or not there is a light mediator between DM and the target nuclei. This can be seen in the WIMP structure factor, although the boost effects on the other hand somewhat cancel it out. The contact interaction leads to a constant cross section, and the exclusion region is horizontal (as shown in the results of Borexino [8]). Our results indicate two distinct regions of momentum dependence: the shape of the lower limits is comparable to those from the WIMP structure factor but with an overall difference of two orders of magnitude when $m_\chi \gtrsim 40$ GeV; below 40 MeV, the exclusion region is modified to a considerably larger value canceling the momentum dependence.

The value m_χ dominates the suppression factor when $m_\chi \gtrsim 40$ GeV, according to numerical results, whereas T_χ^z dominates in the $m_\chi \lesssim 40$ GeV region. This is owing to the fact that the typical transfer momentum q is around 4 ~ 100 MeV. This means the confined quarks in the nucleon can cause the physics of DM detection to differ significantly from the ordinary nonrelativistic scenario. Equivalently, the finite nuclear size effects lead to momentum dependence in the scattering.

IV. CONCLUSION

The ongoing search for dark matter is of critical importance to modern physics. In this paper, we provide the first comprehensive treatment of spin-dependent scattering of BDM, a type of dark matter where the usual nonrelativistic approximations are not reliable.

We found that when the DM is light, the spatial contribution of the boosted structure factor can be much smaller than the WIMP structure factor, while the time component contribution can boost the proton structure factor when the momentum transfer is large enough. We also discovered that, even in the absence of a mediator between dark matter and nuclei target, finite nuclear size effects lead to a residual momentum transfer effect. The complexity in the calculations of the novel boosted structure factor arises because it not only depends on the transfer of momentum q but also the incoming DM momentum.

This new structure factor was applied to the CRDM scenario, providing novel insight into light DM detection. In particular, we showed that the exclusion limits can differ by as much as six orders of magnitude from those calculated using the ordinary nonrelativistic paradigm. Our findings would give conceivable hints on the future search for the light dark matter.

ACKNOWLEDGMENTS

We thank Nick Houston for useful discussions on the manuscript. This work was supported by the Natural Science Foundation of China under Grants No. 12275134, No. 11775012, and No. 11805161.

APPENDIX A: AXIAL-VECTOR CURRENT OF INCOMING DARK MATTER PARTICLES

We adopt the two-component spinor conventions from Ref. [39] in our calculation. The general axial-vector current of Majorana fermion is given by

$$\begin{aligned}
j^\mu(x) &= \bar{u}(p_f, s_f) \gamma^\mu \gamma^5 u(p_i, s_i), \\
&= (y_f \quad x_f^\dagger) \begin{pmatrix} 0 & \sigma^\mu \\ -\bar{\sigma}^\mu & 0 \end{pmatrix} \begin{pmatrix} x_i \\ y_i^\dagger \end{pmatrix}, \\
&= (-x_f^\dagger \bar{\sigma}^\mu x_i + y_f \sigma^\mu y_i^\dagger), \\
&= -\chi_{s_f}^\dagger \sqrt{p_f \cdot \bar{\sigma}} \bar{\sigma}^\mu \sqrt{p_i \cdot \bar{\sigma}} \chi_{s_i} \\
&\quad + \chi_{s_f}^\dagger \sqrt{p_f \cdot \bar{\sigma}} \sigma^\mu \sqrt{p_i \cdot \bar{\sigma}} \chi_{s_i},
\end{aligned} \tag{A1}$$

where x , x^\dagger , y , and y^\dagger are the two-component spinors and $s_{i,f} = \pm \frac{1}{2}$. The relevant basis of two-component spinors χ_s are eigenstates of $\frac{1}{2} \mathbf{p} \cdot \mathbf{s}$. In the nonrelativistic limit,

$$j^\mu(x) = -4s_i s_f m_\chi Z_{-s_i, -s_f}^\mu(\mathbf{p}_f, \mathbf{p}_i) + m_\chi Z_{s_f, s_i}^\mu(\mathbf{p}_f, \mathbf{p}_i), \tag{A2}$$

with

$$Z_{s_i s_f}^\mu(\mathbf{p}_i, \mathbf{p}_f) = \begin{cases} \delta_{s_i s_f} + \left(\frac{p_i}{2m_i} + \frac{p_f}{2m_f} \right) \cdot s^a \tau_{s_i s_f}^a & \mu = 0 \\ s^{a\alpha} \tau_{s_i s_f}^a + \left(\frac{p_i^\alpha}{2m_i} + \frac{p_f^\alpha}{2m_f} \right) \delta_{s_i s_f} + \left(\frac{p_i^\beta}{2m_i} - \frac{p_f^\beta}{2m_f} \right) i e^{\alpha\beta\gamma} s^{a\gamma} \tau_{s_i s_f}^a & \mu = \alpha = 1, 2, 3, \end{cases} \tag{A3}$$

where τ^a are the matrix elements of the Pauli matrices. We use the symbol τ rather than σ to emphasize that the indices of the Pauli matrices τ^a are spin labels s_i, s_f . Then one can easily get the time component of dark matter axial current

$$j^0(x) = -4s_i s_f m_\chi \left[\delta_{-s_i, -s_f} + \left(\frac{p_i}{2m_\chi} + \frac{p_f}{2m_\chi} \right) \cdot s^a \tau_{-s_i, -s_f}^a \right] + m_\chi \left[\delta_{s_i, s_f} + \left(\frac{p_i}{2m_\chi} + \frac{p_f}{2m_\chi} \right) \cdot s^a \tau_{s_i, s_f}^a \right]. \tag{A4}$$

We can see that the momentum term is subleading in case of a low velocity and the mass terms cancel each other after summation of the spins. However, it is also evident that the time component of the axial current of dark matter becomes significant in the relativistic limit

$$j^0(x) = -\chi_{s_f}^\dagger \frac{(E_f + m_\chi) \boldsymbol{\sigma} \cdot \mathbf{p}_i + (E_i + m_\chi) \boldsymbol{\sigma} \cdot \mathbf{p}_f}{\sqrt{(E_f + m_\chi)(E_i + m_\chi)}} \chi_{s_i}. \tag{A5}$$

Thus, the time component of the axial current cannot be neglected in the calculation of the cross sections when the incoming dark matter is relativistic.

Next we give the proof of orthogonality of spatial and time component. The time and spatial components of axial current of dark matter are shown, respectively,

$$j^0 = -x_{(p_f, s_f)}^\dagger x_{(p_i, s_i)} + y_{(p_f, s_f)} y_{(p_i, s_i)}^\dagger, \tag{A6}$$

$$j^i = x_{(p_f, s_f)}^\dagger \boldsymbol{\sigma} x_{(p_i, s_i)} + y_{(p_f, s_f)} \boldsymbol{\sigma} y_{(p_i, s_i)}^\dagger. \tag{A7}$$

The interference of time component and spatial component

$$\begin{aligned}
& \frac{1}{2} \sum_{s_i, s_f} \left(-x_{(p_f, s_f)}^\dagger x_{(p_i, s_i)} + y_{(p_f, s_f)} y_{(p_i, s_i)}^\dagger \right) \left(x_{(p_i, s_i)}^\dagger \boldsymbol{\sigma} x_{(p_f, s_f)} + y_{(p_i, s_i)} \boldsymbol{\sigma} y_{(p_f, s_f)}^\dagger \right) \\
&= \frac{1}{2} \sum_{s_i, s_f} -x_{(p_f, s_f)}^\dagger p_i \cdot \boldsymbol{\sigma} x_{(p_f, s_f)} - x_{(p_f, s_f)}^\dagger m_\chi \boldsymbol{\sigma} y_{(p_f, s_f)}^\dagger + y_{(p_f, s_f)} m_\chi \boldsymbol{\sigma} x_{(p_f, s_f)} + y_{(p_f, s_f)} p_i \cdot \bar{\boldsymbol{\sigma}} y_{(p_f, s_f)}^\dagger \\
&= \frac{1}{2} \text{Tr} [(-p_f \cdot \boldsymbol{\sigma} p_i \cdot \boldsymbol{\sigma} - m_\chi^2 \boldsymbol{\sigma} + m_\chi^2 \bar{\boldsymbol{\sigma}} + p_f \cdot \bar{\boldsymbol{\sigma}} p_i \cdot \bar{\boldsymbol{\sigma}})] \\
&= 0.
\end{aligned} \tag{A8}$$

APPENDIX B: THE SPATIAL COMPONENT OF THE STRUCTURE FACTOR $S_A^0(\mathbf{q})$

We begin our calculation from the scattering amplitude

$$\langle f | \mathcal{L}_\chi^{\text{SD}} | i \rangle = -\frac{G_v}{\sqrt{2}} \int d^3 \mathbf{r} e^{-i\mathbf{q} \cdot \mathbf{r}} \bar{\chi}_f \boldsymbol{\gamma} \boldsymbol{\gamma}_5 \chi_i \mathbf{J}_i^A(\mathbf{r}). \tag{B1}$$

The currents are expanded in terms of spherical unit vectors [40]:

$$\bar{\chi}_f \boldsymbol{\gamma} \boldsymbol{\gamma}_5 \chi_i e^{-i\mathbf{q} \cdot \mathbf{r}} = \mathbf{l} e^{-i\mathbf{q} \cdot \mathbf{r}} = \sum_{\lambda=0, \pm 1} l_\lambda \mathbf{e}_\lambda^\dagger e^{-i\mathbf{q} \cdot \mathbf{r}}, \tag{B2}$$

with spherical unit vectors with a z axis in the direction of \mathbf{q}

$$\mathbf{e}_{\pm 1} \equiv \mp \frac{1}{\sqrt{2}} (\mathbf{e}_{q1} \pm i \mathbf{e}_{q2}) \quad \mathbf{e}_0 \equiv \frac{\mathbf{q}}{q}, \tag{B3}$$

$$l_{\pm 1} = \mp \frac{1}{\sqrt{2}} (l_1 \pm i l_2) \quad l_{\lambda=0} \equiv l_3. \tag{B4}$$

We can also expand the product $\mathbf{e}_\lambda^\dagger e^{-i\mathbf{q} \cdot \mathbf{r}}$ in Eq. (B2) in a multipole expansion [40]. This leads to

$$\begin{aligned}
\langle f | \mathcal{L}_\chi^{\text{SD}} | i \rangle &= -\frac{G_v}{\sqrt{2}} \langle J_f M_f | \left(\sum_{L \geq 0} \sqrt{4\pi(2L+1)} (-i)^L l_3 \mathcal{L}_{L0}^5(\mathbf{q}) \right. \\
&\quad \left. - \sum_{L \geq 1} \sqrt{2\pi(2L+1)} (-i)^L \sum_{\lambda=\pm 1} l_\lambda \right. \\
&\quad \left. \times \left[\mathcal{T}_{L-\lambda}^{\text{el5}}(\mathbf{q}) + \lambda \mathcal{T}_{L-\lambda}^{\text{mag5}}(\mathbf{q}) \right] | J_i M_i \rangle \right)
\end{aligned} \tag{B5}$$

in which $|J_i M_i\rangle$, $|J_f M_f\rangle$ denote the initial and final states of the nuclei, $q = |\mathbf{q}|$.

The electric longitudinal, electric transverse, and magnetic transverse multipole operators are defined by

$$\mathcal{L}_{LM}^5(\mathbf{q}) = \frac{i}{q} \int d^3 \mathbf{r} [\nabla [j_L(qr) \mathbf{Y}_{LM}(\boldsymbol{\Omega}_r)]] \cdot \mathbf{J}^A(\mathbf{r}), \tag{B6}$$

$$\mathcal{T}_{LM}^{\text{el5}}(\mathbf{q}) = \frac{1}{q} \int d^3 \mathbf{r} [\nabla \times j_L(qr) \mathbf{Y}_{LM}^M(\boldsymbol{\Omega}_r)] \cdot \mathbf{J}^A(\mathbf{r}), \tag{B7}$$

$$\mathcal{T}_{LM}^{\text{mag5}}(\mathbf{q}) = \int d^3 \mathbf{r} [j_L(qr) \mathbf{Y}_{LL1}^M(\boldsymbol{\Omega}_r)] \cdot \mathbf{J}^A(\mathbf{r}), \tag{B8}$$

with spherical Bessel function $j_L(qr)$. The vector spherical harmonics are given by

$$\mathbf{Y}_{LL'1}^M(\boldsymbol{\Omega}_r) = \sum_{m\lambda} \langle L' m 1 \lambda | L' 1 LM \rangle Y_{L'm}(\boldsymbol{\Omega}_r) \mathbf{e}_\lambda. \tag{B9}$$

Since $\mathbf{J}^A(\mathbf{r}) = \sum_{i=1}^A \mathbf{J}_i^A(\mathbf{r}) \delta(\mathbf{r} - \mathbf{r}_i)$, the multipole operators can be written as a sum of one-body operators:

$$\begin{aligned}
\mathcal{L}_{LM}^5(\mathbf{q}) &= \frac{i}{q} \sum_{i=1}^A [\nabla [j_L(qr_i) \mathbf{Y}_{LM}(\mathbf{r}_i)]] \cdot \mathbf{J}_i^A(\mathbf{r}_i), \\
&= \frac{i}{\sqrt{2L+1}} \sum_{i=1}^A [\sqrt{L+1} j_{L+1}(qr_i) \mathbf{Y}_{L(L+1)1}^M(\mathbf{r}_i) \\
&\quad + \sqrt{L} j_{L-1}(qr_i) \mathbf{Y}_{L(L-1)1}^M(\mathbf{r}_i)] \cdot \mathbf{J}_i^A(\mathbf{r}_i),
\end{aligned} \tag{B10}$$

$$\begin{aligned}
\mathcal{T}_{LM}^{\text{el5}}(\mathbf{q}) &= \frac{1}{q} \sum_{i=1}^A [\nabla \times j_L(qr_i) \mathbf{Y}_{LL1}^M(\mathbf{r}_i)] \cdot \mathbf{J}_i^A(\mathbf{r}_i), \\
&= \frac{i}{\sqrt{2L+1}} \sum_{i=1}^A \left[\sqrt{L+1} j_{L-1}(qr_i) \mathbf{Y}_{L(L-1)1}^M(\mathbf{r}_i) \right. \\
&\quad \left. - \sqrt{L} j_{L+1}(qr_i) \mathbf{Y}_{L(L+1)1}^M(\mathbf{r}_i) \right] \cdot \mathbf{J}_i^A(\mathbf{r}_i),
\end{aligned} \tag{B11}$$

$$\mathcal{T}_{LM}^{\text{mag5}}(\mathbf{q}) = \sum_{i=1}^A j_L(qr_i) \mathbf{Y}_{LL1}^M(\mathbf{r}_i) \cdot \mathbf{J}_i^A(\mathbf{r}_i). \tag{B12}$$

The structure factor $S_A(q)$ is obtained from $|\langle f | \mathcal{L}_\chi^{\text{SD}} | i \rangle|^2$ by summing over the final DM spin and over the DM final-state angular momentum projections and by averaging over the initial configurations. It is thus useful to work with reduced matrix elements that do not depend on projection numbers:

$$\langle J_f M_f | O_{LM} | J_i M_i \rangle = (-1)^{J_f - M_f} \begin{pmatrix} J_f & L & J_i \\ -M_f & M & M_i \end{pmatrix} \langle J_f || O_L || J_i \rangle, \quad (\text{B13})$$

with $3j$ coefficients and where O is a tensor operator of rank L . This gives for the sum and average [40]

$$\begin{aligned} \frac{1}{2(2J_i + 1)} \sum_{s_f, s_i} \sum_{M_f, M_i} |\langle f | \mathcal{L}_\chi^{\text{SD}} | i \rangle|^2 &= \frac{\pi G_v^2}{(2J_i + 1)} \sum_{s_f, s_i} \left(\sum_{L \geq 0} l_3 l_3^* |\langle J_f || \mathcal{L}_L^5 || J_i \rangle|^2 + \sum_{L \geq 1} \left[\frac{1}{2} (\mathbf{1} \cdot \mathbf{1}^* - l_3 l_3^*) (|\langle J_f || \mathcal{T}_L^{\text{el}5} || J_i \rangle|^2 \right. \right. \\ &\quad \left. \left. + |\langle J_f || \mathcal{T}_L^{\text{mag}5} || J_i \rangle|^2) - \frac{i}{2} (\mathbf{1} \times \mathbf{1}^*)_3 (2 \text{Re} \langle J_f || \mathcal{T}_L^{\text{el}5} || J_i \rangle \langle J_f || \mathcal{T}_L^{\text{mag}5} || J_i \rangle^*) \right] \right), \quad (\text{B14}) \end{aligned}$$

where we have assumed that the DM spin is $1/2$, and the cross terms vanish due to the orthogonal properties of the $3j$ coefficients.

For the sum over DM spin projections one has for $\mu, \nu = 1, 2, 3$

$$\begin{aligned} -\sum_{s_i, s_f} l_\mu l_\nu^* &= \sum_{s_i, s_f} \bar{\chi}^{s_f}(p_f) \gamma^\mu \gamma^5 \chi^{s_i}(p_i) \bar{\chi}^{s_i}(p_i) \gamma^5 \gamma^\nu \chi^{s_f}(p_f), \\ &= \sum_{s_i, s_f} (\chi_\delta^{s_f}(p_f) \bar{\chi}_\alpha^{s_f}(p_f) (\gamma^\mu \gamma^5)_{\alpha\beta} \chi_\beta^{s_i}(p_i) \\ &\quad \times \bar{\chi}_\gamma^{s_i}(p_i) (\gamma^5 \gamma^\nu)_{\gamma\delta}), \quad (\text{B15}) \end{aligned}$$

in the nonrelativistic limit

$$\sum_s \chi_\alpha^s(p) \bar{\chi}_\beta^s(p) \approx \frac{1}{2} (\gamma^0 + 1)_{\alpha\beta}, \quad (\text{B16})$$

thus

$$\begin{aligned} -\sum_{s_i, s_f} l_\mu l_\nu^* &= \frac{1}{4} [2 \text{Tr}(\gamma^0 \gamma^\mu \gamma^5 \gamma^5 \gamma^\nu) + 2 \text{Tr}(\gamma^\mu \gamma^5 \gamma^5 \gamma^\nu)] \\ &= \frac{1}{2} \text{Tr}(\gamma^\mu \gamma^5 \gamma^5 \gamma^\nu) = -2\delta^{\mu\nu}. \quad (\text{B17}) \end{aligned}$$

Then

$$\begin{aligned} \frac{1}{2(2J_i + 1)} \sum_{s_f, s_i} \sum_{M_f, M_i} |\langle f | \mathcal{L}_\chi^{\text{SD}} | i \rangle|^2 \\ &= \frac{G_v^2}{2} \frac{4\pi}{(2J_i + 1)} \left[\sum_{L \geq 0} |\langle J_f || \mathcal{L}_L^5 || J_i \rangle|^2 \right. \\ &\quad \left. + \sum_{L \geq 1} (|\langle J_f || \mathcal{T}_L^{\text{el}5} || J_i \rangle|^2 + |\langle J_f || \mathcal{T}_L^{\text{mag}5} || J_i \rangle|^2) \right]. \quad (\text{B18}) \end{aligned}$$

Finally

$$\begin{aligned} S_A(q) &= \sum_{L \geq 0} |\langle J_f || \mathcal{L}_L^5 || J_i \rangle|^2 + \sum_{L \geq 1} (|\langle J_f || \mathcal{T}_L^{\text{el}5} || J_i \rangle|^2 \\ &\quad + |\langle J_f || \mathcal{T}_L^{\text{mag}5} || J_i \rangle|^2). \quad (\text{B19}) \end{aligned}$$

In case of a fast moving dark matter, the completeness relation is

$$\sum_s \chi_\alpha^s(p) \bar{\chi}_\beta^s(p) = \left(\frac{p_\mu \gamma^\mu + m_\chi}{2E_p} \right)_{\alpha\beta}. \quad (\text{B20})$$

Then

$$\begin{aligned} -\sum_{s_i, s_f} l_\mu l_\nu^* &= \sum_{s_i, s_f} \frac{p_{f\rho} \gamma^\rho + m_\chi}{2E_{p_f}} \gamma^\mu \gamma^5 \frac{p_{i\sigma} \gamma^\sigma + m_\chi}{2E_{p_i}} \gamma^5 \gamma^\nu \\ &= \frac{1}{E_{p_f} E_{p_i}} [-p_f^\mu p_i^\nu - p_f^\nu p_i^\mu + (p_f \cdot p_i + m_\chi^2) g^{\mu\nu}]. \quad (\text{B21}) \end{aligned}$$

Similarly

$$\frac{1}{2(2J_i + 1)} \sum_{s_f, s_i} \sum_{M_f, M_i} |\langle f | \mathcal{L}_\chi^{\text{SD}} | i \rangle|^2 = \frac{G_v^2}{4} \frac{4\pi}{(2J_i + 1)} \left[\sum_{L \geq 0} \frac{1}{E_{p_f} E_{p_i}} (2p_f^3 p_i^3 + p_f \cdot p_i + m_\chi^2) |\langle J_f | \mathcal{L}_L^5 | J_i \rangle|^2 \right. \\ \left. + \sum_{L \geq 1} \frac{1}{E_{p_f} E_{p_i}} (p_f^1 p_i^1 + p_f^2 p_i^2 + p_f \cdot p_i + m_\chi^2) |\langle J_f | (\mathcal{T}_L^{\text{el}5} + \mathcal{T}_L^{\text{mag}5}) | J_i \rangle|^2 \right] \quad (\text{B22})$$

and

$$S_A(q) = \frac{1}{4\pi G_v^2} \sum_{s_f, s_i} \sum_{M_f, M_i} |\langle f | \mathcal{L}_\chi^{\text{SD}} | i \rangle|^2 = \frac{1}{2} \left[\sum_{L \geq 0} \frac{1}{E_{p_f} E_{p_i}} (2p_f^3 p_i^3 + p_f \cdot p_i + m_\chi^2) |\langle J_f | \mathcal{L}_L^5 | J_i \rangle|^2 \right. \\ \left. + \sum_{L \geq 1} \frac{1}{E_{p_f} E_{p_i}} (p_f^1 p_i^1 + p_f^2 p_i^2 + p_f \cdot p_i + m_\chi^2) |\langle J_f | (\mathcal{T}_L^{\text{el}5} + \mathcal{T}_L^{\text{mag}5}) | J_i \rangle|^2 \right]. \quad (\text{B23})$$

The collision between dark matter and nuclei can be chosen in a frame that the incident dark matter with an energy T_χ^z is moving along the Z axis, as shown in the Fig. 3. The recoil direction of the nuclei can be easily got from

$$\cos \theta = \frac{q}{2p_i^3}. \quad (\text{B24})$$

Then for the isotropic incident flux, substituting the recoil angle θ into Eq. (B23) and integrating all the direction of the flux, the structure factor can be written as

$$S_A(q) = \frac{4(T_\chi^z + m_\chi)^2 - q^2}{4(T_\chi^z + m_\chi)^2} \sum_{L \geq 0} |\langle J_f | \mathcal{L}_L^5 | J_i \rangle|^2 \\ + \frac{q^2 + 4m_\chi^2}{4(T_\chi^z + m_\chi)^2} \sum_{L \geq 1} |\langle J_f | (\mathcal{T}_L^{\text{el}5} + \mathcal{T}_L^{\text{mag}5}) | J_i \rangle|^2. \quad (\text{B25})$$

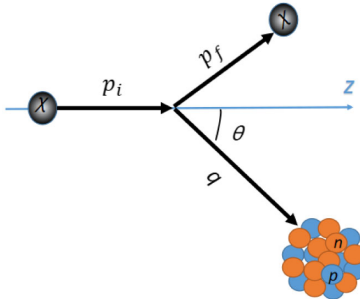


FIG. 3. A collision of the incident dark matter and the nuclei along the Z axis.

APPENDIX C: THE TIME COMPONENT OF THE STRUCTURE FACTOR $S_T(q)$

Time component of the Lagrangian density between the initial and final state is

$$\langle f | \mathcal{L}_\chi^{\text{SD}} | i \rangle = \frac{G_v}{\sqrt{2}} \bar{\chi}_f \gamma_0 \gamma_5 \chi_i J_0^A. \quad (\text{C1})$$

The one-nucleon time component of axial-current matrix element is [41]

$$\langle [N] p'_f, s'_f | J_0^A(x) | [N] p'_i, s'_i \rangle = \bar{U}_N(p'_f, s'_f) \\ \frac{1}{2} [(a_0 + a_1 \tau_3) \gamma_0 \gamma_5 + (b_0 + b_1 \tau_3) q_0 \gamma_5] U_N(p'_i, s'_i), \quad (\text{C2})$$

in which U_N is a nucleon spinor, p'_f, p'_i are the one-shell four momenta and s'_f, s'_i are the spin labels, $q_\mu = (p'_f - p'_i)_\mu$. Note that q^2 is not $q_\mu q^\mu$ but $-q_\mu q^\mu$. The a_0, a_1 are completely determined by the A_q and three number Δq (for $q = u, d$ and s quarks) defined as

$$\Delta q s^\mu = \langle p_f, s_f | \bar{\psi}_q \gamma^\mu \gamma_5 \psi_q | p_f, s_f \rangle, \quad (\text{C3})$$

in which the matrix element is for the proton, and s^μ is the spin vector defined in the usual way [42]. Specifically, the couplings of the isoscalar part and isovector part are

$$a_0 = (A_u + A_d)(\Delta u + \Delta d) + 2A_s \Delta s, \quad (\text{C4})$$

$$a_1 = (A_u - A_d)(\Delta u - \Delta d). \quad (\text{C5})$$

The b coefficients can be estimated from the partially conserved axial-vector current (PCAC) [43], just as they are for the axial weak current. b_0 and b_1 are called isoscale and isovector coefficients, the second term is from the exchange of virtual mesons. The isoscalar mesons are heavy enough to set $b_0 \simeq 0$ and pion exchange induces an isovector coefficient

$$b_1 = \frac{m_N a_1}{q^2 + m_\pi^2}. \quad (\text{C6})$$

Next, the time component of the axial-current matrix at nucleon level should be translated into the nuclear matrix elements. This simply takes the form [40]

$$\langle f | \mathcal{L}_\chi^{\text{SD}} | i \rangle = \frac{G_V}{\sqrt{2}} \int d^3 \mathbf{r} e^{-iq \cdot \mathbf{r}} \bar{\chi}_f \gamma_0 \gamma_5 \chi_i \rho(\mathbf{r}), \quad (\text{C7})$$

in which $\rho(\mathbf{r})$ is the charge distribution density of axial current in a nuclei. However, as far as we know, the axial charge distributions in the nuclei still lack experimental data. Thus in our paper, we take the one nucleon time component contributions to account for the contributions at nuclear level for the simplicity. Summing the final state and averaging the initial state, we have

$$\begin{aligned} \frac{1}{4} \sum_{s'_f, s'_i} \sum_{s_f, s_i} |\langle f | \mathcal{L}_\chi^{\text{SD}} | i \rangle|^2 &= \frac{1}{4E_i E_f} \frac{1}{4E'_i E'_f} \frac{G_V^2}{2} \left[(a_0 + a_1 \tau_3)^2 \left(2E_i E_f - \frac{q^2}{2} - 2m_\chi^2 \right) \left(2E'_i E'_f - \frac{q^2}{2} - 2m_N^2 \right) \right. \\ &\quad + 2(a_0 + \tau_3)(b_0 + b_1 \tau_3) \left(2E_i E_f - \frac{q^2}{2} - 2m_\chi^2 \right) (E'_i - E'_f) m_N q_0 \\ &\quad \left. + (b_0 + b_1 \tau_3)^2 \left(2E_i E_f - \frac{q^2}{2} - 2m_\chi^2 \right) \frac{q^2}{2} q_0^2 \right], \end{aligned} \quad (\text{C8})$$

which are referred to as “proton-only.” It is defined by the couplings $a_0 = a_1 = 1$, $\tau_3 = 1$. Thus, in the case of protons only,

$$\begin{aligned} \frac{1}{4} \sum_{s'_f, s'_i} \sum_{s_f, s_i} |\langle f | \mathcal{L}_\chi^{\text{SD}} | i \rangle|^2 &= \frac{1}{4E_i E_f} \frac{1}{4E'_i E'_f} \frac{G_V^2}{2} \left[4 \left(2E_i E_f - \frac{q^2}{2} - 2m_\chi^2 \right) \left(2E'_i E'_f - \frac{q^2}{2} - 2m_N^2 \right) \right. \\ &\quad \left. + 4 \frac{m_N}{q^2 + m_\pi^2} \left(2E_i E_f - \frac{q^2}{2} - 2m_\chi^2 \right) (E'_i - E'_f) m_N q_0 + \left(\frac{m_N}{q^2 + m_\pi^2} \right)^2 \left(2E_i E_f - \frac{q^2}{2} - 2m_\chi^2 \right) \frac{q^2}{2} q_0^2 \right], \end{aligned} \quad (\text{C9})$$

$$\begin{aligned} S_T(q) &= \frac{1}{4\pi G_V^2} \sum_{s'_f, s'_i} \sum_{s_f, s_i} |\langle f | \mathcal{L}_\chi^{\text{SD}} | i \rangle|^2 = \frac{1}{4E_i E_f} \frac{1}{4E'_i E'_f} \frac{1}{2\pi} \left[4 \left(2E_i E_f - \frac{q^2}{2} - 2m_\chi^2 \right) \left(2E'_i E'_f - \frac{q^2}{2} - 2m_N^2 \right) \right. \\ &\quad \left. + 4 \frac{m_N}{q^2 + m_\pi^2} \left(2E_i E_f - \frac{q^2}{2} - 2m_\chi^2 \right) (E'_i - E'_f) m_N q_0 + \left(\frac{m_N}{q^2 + m_\pi^2} \right)^2 \left(2E_i E_f - \frac{q^2}{2} - 2m_\chi^2 \right) \frac{q^2}{2} q_0^2 \right]. \end{aligned} \quad (\text{C10})$$

-
- [1] G. Bertone, D. Hooper, and J. Silk, *Phys. Rep.* **405**, 279 (2005).
[2] M. Battaglieri *et al.*, arXiv:1707.04591.
[3] M. Ibe, W. Nakano, Y. Shoji, and K. Suzuki, *J. High Energy Phys.* **03** (2018) 194.
[4] M. J. Dolan, F. Kahlhoefer, and C. McCabe, *Phys. Rev. Lett.* **121**, 101801 (2018).
[5] V. V. Flambaum, L. Su, L. Wu, and B. Zhu, arXiv:2012.09751.
[6] S. Knapen, J. Kozaczuk, and T. Lin, *Phys. Rev. Lett.* **127**, 081805 (2021).
[7] H. An, M. Pospelov, J. Pradler, and A. Ritz, *Phys. Rev. Lett.* **120**, 141801 (2018); **121**, 259903(E) (2018).
[8] T. Bringmann and M. Pospelov, *Phys. Rev. Lett.* **122**, 171801 (2019).
[9] Y. Ema, F. Sala, and R. Sato, *Phys. Rev. Lett.* **122**, 181802 (2019).
[10] D. McKeen and N. Raj, *Phys. Rev. D* **99**, 103003 (2019).
[11] J. Alvey, M. Campos, M. Fairbairn, and T. You, *Phys. Rev. Lett.* **123**, 261802 (2019).
[12] J. B. Dent, B. Dutta, J. L. Newstead, and I. M. Shoemaker, *Phys. Rev. D* **101**, 116007 (2020).
[13] W. Wang, L. Wu, J. M. Yang, H. Zhou, and B. Zhu, *J. High Energy Phys.* **12** (2020) 072.
[14] S.-F. Ge, J.-L. Liu, Q. Yuan, and N. Zhou, *Phys. Rev. Lett.* **126**, 091804 (2021).

- [15] L. Su, W. Wang, L. Wu, J. M. Yang, and B. Zhu, *Phys. Rev. D* **102**, 115028 (2020).
- [16] C. Xia, Y.-H. Xu, and Y.-F. Zhou, *Nucl. Phys.* **B969**, 115470 (2021).
- [17] G. Guo, Y.-L. S. Tsai, M.-R. Wu, and Q. Yuan, *Phys. Rev. D* **102**, 103004 (2020).
- [18] G. Herrera and A. Ibarra, *Phys. Lett. B* **820**, 136551 (2021).
- [19] N. F. Bell, J. B. Dent, B. Dutta, S. Ghosh, J. Kumar, J. L. Newstead, and I. M. Shoemaker, *Phys. Rev. D* **104**, 076020 (2021).
- [20] E. Del Nobile, *The Theory of Direct Dark Matter Detection: A Guide to Computations* (Springer, Cham, 2022).
- [21] J.-C. Feng, X.-W. Kang, C.-T. Lu, Y.-L. S. Tsai, and F.-S. Zhang, *J. High Energy Phys.* **04** (2022) 080.
- [22] H. Kolesova, [arXiv:2209.14600](https://arxiv.org/abs/2209.14600).
- [23] J. Alvey, T. Bringmann, and H. Kolesova, *J. High Energy Phys.* **01** (2023) 123.
- [24] Z.-H. Lei, J. Tang, and B.-L. Zhang, *Chin. Phys. C* **46**, 085103 (2022).
- [25] S. Chang, A. Pierce, and N. Weiner, *J. Cosmol. Astropart. Phys.* **01** (2010) 006.
- [26] S. P. Martin, *Adv. Ser. Dir. High Energy Phys.* **18**, 1 (1998).
- [27] C. Csaki, J. Hubisz, and P. Meade, in *Theoretical Advanced Study Institute in Elementary Particle Physics: Physics in $D \geq 4$* (2005), pp. 703–776.
- [28] P. Klos, J. Menéndez, D. Gazit, and A. Schwenk, *Phys. Rev. D* **88**, 083516 (2013); **89**, 029901(E) (2014).
- [29] F. Bishara, J. Brod, B. Grinstein, and J. Zupan, [arXiv:1708.02678](https://arxiv.org/abs/1708.02678).
- [30] E. Aprile *et al.* (XENON Collaboration), *Phys. Rev. Lett.* **122**, 141301 (2019).
- [31] S. Della Torre *et al.*, [arXiv:1612.08445](https://arxiv.org/abs/1612.08445).
- [32] T. Bringmann, J. Edsjö, P. Gondolo, P. Ullio, and L. Bergström, *J. Cosmol. Astropart. Phys.* **07** (2018) 033.
- [33] P. Gondolo, J. Edsjo, P. Ullio, L. Bergstrom, M. Schelke, and E. A. Baltz, *J. Cosmol. Astropart. Phys.* **07** (2004) 008.
- [34] The Darksusy package can be downloaded from following website: <https://darksusy.hepforge.org>. Our modifications on the package can be found in <https://github.com/wennayang/DarkSUSY-6.3.1-.git>.
- [35] R. Agnese *et al.* (SuperCDMS Collaboration), *Phys. Rev. D* **97**, 022002 (2018).
- [36] C. Amole *et al.* (PICO Collaboration), *Phys. Rev. Lett.* **118**, 251301 (2017).
- [37] M. G. Aartsen *et al.* (IceCube and PICO Collaborations), *Eur. Phys. J. C* **80**, 819 (2020).
- [38] J. I. Collar, *Phys. Rev. D* **98**, 023005 (2018).
- [39] H. K. Dreiner, H. E. Haber, and S. P. Martin, *Phys. Rep.* **494**, 1 (2010).
- [40] J. D. Walecka, *Theoretical Nuclear and Subnuclear Physics* (1995), Vol. 16.
- [41] J. Engel, S. Pittel, and P. Vogel, *Int. J. Mod. Phys. E* **1**, 1 (1992).
- [42] R. L. Jaffe and A. Manohar, *Nucl. Phys.* **B337**, 509 (1990).
- [43] C. Chen, C. S. Fischer, C. D. Roberts, and J. Segovia, *Phys. Rev. D* **105**, 094022 (2022).